TPM Vol. 32, No. S8, 2025
ISSN: 1972-6325
https://www.tpmap.org/

Open Access

# MGSO4-DOPED-ADDITIVE TIO2 NANOPARTICLE: CO-ACTIVE PROCEDURE TOWARDS REALIZING AN IMPROVED PASSIVATED PHOTOELECTRODE OF DYE-SENSITIZED SOLAR CELLS

A.A. KHAN[1], M.H. ABDULLAH[1]*, R. RADZALI[1], E. NOORSAL[1], M.H. MAMAT[2], A. SUPRIYANTO[3]

[1]SCHOOL OF ELECTRICAL ENGINEERING, COLLEGE OF ENGINEERING, UNIVERSITI TEKNOLOGI MARA, CAWANGAN PULAU PINANG, 13500 PERMATANG PAUH, PULAU PINANG, MALAYSIA
[2]NANO-ELECTRONIC CENTRE (NET), COLLEGE OF ELECTRICAL ENGINEERING, UNIVERSITI TEKNOLOGI MARA, 40450 SHAH ALAM, SELANGOR, MALAYSIA
[3]DEPARTMENT OF PHYSICS, GRADUATE PROGRAM, UNIVERSITAS SEBELAS MARET, ST. IR. SUTAMI 36A KENTINGAN JEBRES, SURAKARTA 57126, INDONESIA

**ABSTRACT**
The application of a passivation layer on the titanium dioxide ($TiO_2$) photoelectrode, along with the treatment of dye sensitizers utilizing dye additives, represents two fundamental approaches utilized to enhance the efficiency of photogenerated electrons in dye-sensitized solar cells (DSSCs). This study represents a novel exploration into the combined application of $MgSO_4$-doped $TiO_2$ passivation photoelectrodes and $MgSO_4$ dye additives, with a meticulous examination of their collective impact on the performance of dye-sensitized solar cells (DSSCs). The effects of $MgSO_4$ incorporation to $TiO_2$ on the morphological, structural, and optical properties were analyzed using field-emission-SEM (FESEM) and ultraviolet–visible spectroscopy (UV–Vis Spectroscopy). Meanwhile, the effect of $MgSO_4$ dye additive on the functional group of the natural dye sensitizer extracted from Mitragyna speciosa (MS) was investigated using FTIR spectroscopy. Finally, the performances of four different types of solar cells with various treatment procedures were compared. Among the evaluated cells, the double treatments cell involving the $MgSO_4$-doped $TiO_2$ followed with $MgSO_4$ treated dye additive process (i.e, $MgSO_4$-doped $TiO_2$-A) is verified to be superior to others in terms of power conversion efficiency, η and photocurrent density, Jsc of 0.86 %, and 3.38 mA/cm$^2$, respectively. The enhancement in power conversion efficiency can be attributed primarily to the elevated photocurrent density, Jsc, and open circuit voltage, Voc. These factors are intricately linked to the advantages of a passivation layer that reduced recombination as well as lowering interfacial resistance at the cell's interfaces, secondly due to dye additive that improving dye molecules attachment to the $TiO_2$ nanoparticles. The co-active impact has significantly influenced the band structure, charge transport, and recombination processes within the cell.
**Keywords:** DSSC, Dye-additive, Charge transport, $MgSO_4$-doped $TiO_2$, Mitragyna speciosa, Passivation

## 1. INTRODUCTION

Dye-sensitized solar cells (DSSCs) represent a prominent approach to harnessing solar energy, garnering growing interest due to their numerous advantages such as low production cost, high efficiency, flexibility and ease of fabrication if compared to traditional silicon-based solar cells. [1][2][3][4]. In general DSSC devices comprises of photoanode, dye molecule sensitizer, electrolyte, and counter electrode [5]. The photoanode, as the first component of the DSSC, is essential for the attachment of dye molecules and for enabling the processes of electron generation and transfer within the cell. The DSSC employing titanium dioxide ($TiO_2$) as a photoanode has attained notable efficiencies of up to 14% [6][7]. To achieve higher performance photoanode, some modification processes such as $TiO_2$ doping can be employed during the preparation of the photoanode. The purpose of doping is to modify the optical and/or electrical properties of $TiO_2$ thin films, typically achieved through the intentional introduction of metal cations as impurities into the titanium dioxide crystal lattice [8][9][10].
Magnesium, Mg, is an alkaline earth of a divalent metal cation that has been utilized as dopant in $TiO_2$ anatase to enhance photocatalytic activities for various applications, including photocatalysis and DSSCs [11][12]. From an atomic standpoint, the Mg cation (0.72 Å) possesses a slightly larger atomic radius compared to the Ti cation (0.64 Å), which positions Mg as a favourable option for doping to modify bandgap alignment of the final composition [13]. Moreover, Mg has a lower conduction band (CB) than $TiO_2$ which results in squeezing the conduction-band, CB of $TiO_2$ thereby, enhancing the photo absorption [12]. Again, Mg is the most popular p-type dopant for enhancing the optoelectrical effect of gallium nitride (GaN), a widely used material for blue light-

emitting diodes, as well as zinc oxide thin film modification for sol–gel technique applications [14]. It is also reported that Mg doping is applied in positive electrode materials rich in nickel for Li batteries to hinder the Ni migration into the Li layer and increase capacity retention [15]. Furthermore, due to the similarity in the ionic radius of $Mg^{2+}$ and $Li^{+}$ ions made it a good choice as the dopant element. From another standpoint, particularly regarding the dye additive, the benefits of this additive have been documented by numerous studies. We have documented multiple investigations employing various salt materials for dye additive, including $Al_2(SO_4)_3$ and $MgSO_4$ [21,32]. Based on the findings of those investigations, it has been observed that the addition of dye showed a remarkable improvement in photocatalytic activity, dye adsorption on $TiO_2$ nanoparticles, and protonation level, all of which ultimately contributed to the performance of the cell.

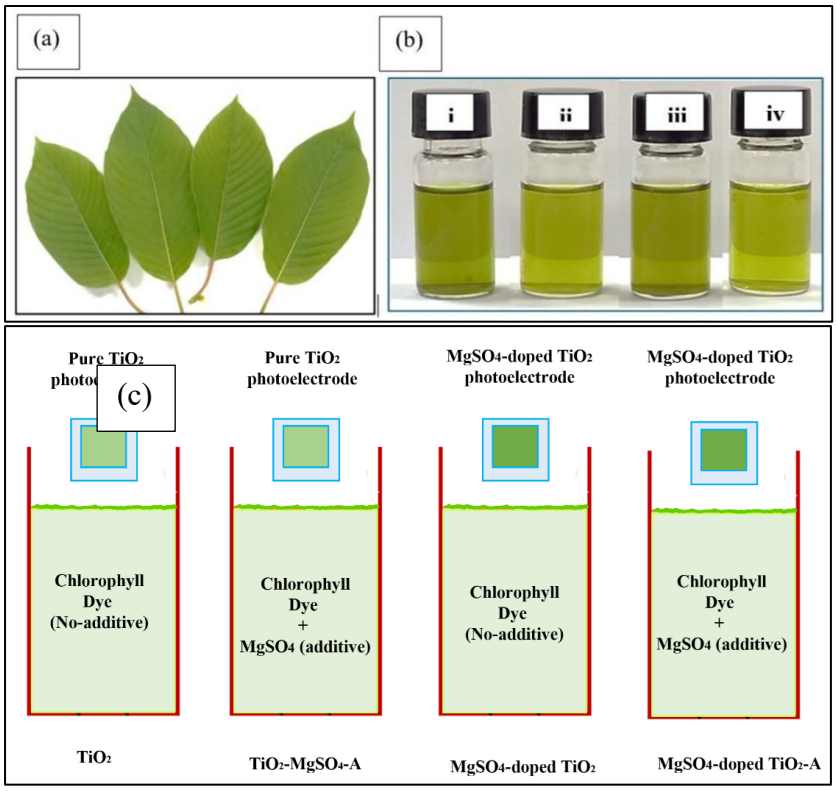


**Fig. 1. (a)** Fresh MS leaves **(b)** various types of dye solutions (after immersed with each electrode) **(c)** Four different types of photoelectrodes investigated in this study

Figure 1(a) presents the fresh sample of MS leaves utilized in this investigation. In the meantime, different samples of the dye solutions after immersion are presented in Figure 1(b). Figure 1(c) illustrates four distinct types of $TiO_2$ photoelectrodes developed through the experimental procedure, labeled as follows: $TiO_2$ (pure $TiO_2$), $TiO_2$ with additive ($TiO_2$ -$MgSO_4$-A), magnesium sulfate-doped without additive ($MgSO_4$-doped $TiO_2$), and magnesium sulfate-doped $TiO_2$ with $MgSO_4$ additive ($MgSO_4$-doped $TiO_2$ -A). Apart from the $TiO_2$ photoanode, this research utilized dye molecule sensitizer extracted from fresh leaves of Mitragyna speciosa (MS), which is part of the Rubiaceae family and the Naucleeae tribe. The leaves are known as kratom or ketum in Southeast Asia, particularly Thailand and Malaysia, while in Western countries, "kratom" is the predominant name. The native ecological habitat for kratom is wet and rich soils, with medium to full sun exposure zones and high doses of ultraviolet (UV) light [16]. Ghazali et al. [17] performed experimental analysis to investigate the pigment extracted from kratom leaves. The authors reported kratom leaves contain highest alkaloid contents and its leaves have a high concentration of chlorophylls. Chlorophylls are green-coloured macrocyclic pigments and the primary photosynthetic pigments in nature [18]. Furthermore, chlorophylls can be considered as ideal photosensitisers in DSSC due to their highly stable polycyclic network of alternating single and double bonds (polyenes) conjugated structure, that allows the orbitals delocalization [8]. Nevertheless, making chlorophylls as a potential source of eco-friendly dye in numerous studies [19]. Moreover, Calogero and co-workers highlights that cells treated with chlorophyll derivatives as sensitisers have a conversion efficiency of more than 2% [20].

Following the successful establishment of $MgSO_4$ as the dye additive for the MS dye in our previous study [21]. In this present research we investigated the combined effect of co-active procedure (passivation layer and dye treatment using $MgSO_4$) through $MgSO_4$-doped-immersed $TiO_2$ (i.e. $MgSO_4$-doped $TiO_2$ nanoparticles then immersed in the $MgSO_4$-treated dye solution) which is denoted as $MgSO_4$-doped $TiO_2$-A. To the best of our knowledge, the co-active approach of $MgSO_4$-doped $TiO_2$ -A photoelectrode utilized in DSSC represents the inaugural instance of this investigation. Firstly, the structural, surface morphology, optical and electrical properties of $MgSO_4$-$TiO_2$ thin films. were characterized using FESEM, EDX and UV-Vis spectroscopy. The functional group and chemical bonding of the treated and untreated chlorophyll dyes were analysed using FTIR.

Finally, the current density-voltage (I-V) characteristics was measured and analysed under AM 1.5 illumination with 100 mW/cm$^2$ light intensity to evaluate the performance of MS dye for each sample.

## 2. Experimental Procedure

### 2.1 Materials

Indium tin oxide (ITO) conducting glass plates (1 mm thick, 80% transparency; was obtained from Biotin Glass Co. Titanium dioxide ($TiO_2$) nano-powders (99.7% purity, P25, particle size: <25 nm), Tetrabutylammonium iodide (TBAI) (electrolyte), acetonitrile (98%), iodine ($I_2$) was obtained from Aldrich Co. A magnesium sulfate ($MgSO_4$) crystalline solid was supplied from Sigma Aldrich, which was used as both an additive and doping. Methanol (99%) was purchased from QRëC. Acetic acid (98%) was obtained from Merck & Co. Filter paper (Whatman, No. 1) and was purchased from Modern Lab. Meanwhile, the digital multimeter (Model: RS 14) was purchased from RS PRO and the ultrasonic bath (Digital Ultrasonic Cleaner: Model: PS-40A) was obtained from Alibaba.com, respectively. Magnetic stirrer (RET Basic) was purchased from IKA Magnetic Stirrers and (Hamilton Beach Commercial, Model: HBB909). Finally, MS leaves used as a natural dye were obtained from a local supplier in Pulau Pinang, Malaysia. All materials were used without further purification.

### 2.2 Preparation of natural plant

Fresh Mitragyna speciosa (MS) leaves were collected from the local licensed supplier from the district of Seberang Perai, Pulau Pinang, Malaysia. The leaves were authenticated by certified botanist, Dr. Farah Alia Binti Nordin, from the School of Biological Sciences, University Science Malaysia (USM), Malaysia. The voucher specimen No. is 11074. The leaves were cleansed with de-ionized water (DI) and allowed to naturally dry at room temperature before being crushed using a grinder (Hamilton Beach Commercial, Model: HBB909). Then, 40 grams of ground MS leaves were dispersed in 50 ml of methanol (100%, v/v) and the mixture was stirred using a magnetic stirrer to facilitate the dissolution of chlorophyll in methanol. Afterwards, filtration process was carried out using filter paper (Whatman, No. 1) and the filtered dye solution was divided into four beakers. Then, the dye solution was completely dissolved in two beakers with 0.3 g of $MgSO_4$ each and denoted as $TiO_2$-$MgSO_4$-A and $MgSO_4$- doped $TiO_2$-A, respectively. The remaining dye solutions were denoted as $TiO_2$ and $MgSO_4$-doped $TiO_2$. In the preparation of photoelectrodes, ITO-coated $TiO_2$ with and without additive ($TiO_2$ and $TiO_2$-A) and ITO-coated magnesium-doped with and without additive ($MgSO_4$-doped $TiO_2$ and $MgSO_4$-doped $TiO_2$) were finally submerged in their respective dye sensitiser solutions.

### 2.3 Preparation of conductive ITO glass

Indium tin oxide (ITO) glass substrates (2.5 cm x 2.5 cm, 8 Ω/sq) were utilized as anode and cathode. The conductive side of the ITO glasses was identified using a digital multimeter. The ITO conducting substrates were first cleaned in an ultrasonic bath with acetone for 20 min. After that, the ITO glass substrates were rinsed with distilled water to remove any mineral traces before air drying at room temperature.

For the preparation of undoped $TiO_2$ and magnesium-doped $TiO_2$ ($MgSO_4$- doped $TiO_2$): The undoped and magnesium-doped $TiO_2$ pastes were prepared using 2 g of anatase powder, 5 mL of DI water, and 1 mL of acetic acid and 1 mL of diluted detergent. Typically, 1 mL of acetic acid was mixed with 5 ml of DI water and continuously stirred until the solution was homogeneous, using a stirrer. Then, the solution was poured into 2 g of $TiO_2$ powder and stirred for 8-10 min to obtain a homogenous mixture. Finally, 1 mL of diluted detergent was added to the paste and stirred until it was smooth and lump-free. To avoid bubbles, the mixture was slowly stirred at a low speed. The method for the magnesium-doped procedure was similar to the above, the only difference is that for the first step, 0.03 g of $MgSO_4$ was dissolved in a 5:1 volume ratio of DI water and acetic acid and stirred until complete dissolution and homogeneity were attained. Both pastes were sonicated for 30 min to form a good coating and required to be stored for at least one night before being utilised as photoelectrode in DSSC.

### 2.4 Electrolyte preparation

The iodine/triiodide electrolyte was synthesized following the methodology outlined in a prior investigation [22]. In general, the liquid iodine was prepared by utilizing a colloidal suspension consisting of 0.127 g of granule iodine (I2), 0.83 g of Tetrabutylammonium iodide (TBAI), and 10 ml of acetonitrile.

### 2.5 Preparation of counter electrode

Graphite from 2B pencil lead (Faber Castell) was used as catalytic material on the conducting sides of the ITO glass [23].

### 2.6 Photoelectrodes and DSSC fabrication

To prepare the $TiO_2$ photoelectrodes, a region of 1 cm × 1 cm was patterned with scotch tape, and a suitable amount of $TiO_2$ paste was deposited on the glass substrate using the Dr Blade technique. Then, the ITO substrates were placed in a tubular furnace (Nabertherm Universal Tube Furnace, B180). The prepared films were annealed at 550 °C for 40 min. The $TiO_2$ electrodes were then allowed to cool at room temperature to prevent the surface of the thin film from cracking before being removed from the furnace [24]. The prepared photoelectrodes were then immersed in their respective dye solutions for 24 hrs, allowing the dye molecules to be adsorbed on the surface of the $TiO_2$ nanoparticles. Based on the measurement evaluated by a Surface Profiling instrument (Veeco, Dektak 150), the thickness of the prepared $TiO_2$ photoelectrodes was approximately 15 µm. The photoelectrodes were rinsed with methanol and then the two photoelectrodes were finally assembled using binder clips. Finally, an electrolyte was injected into the space between the electrodes. The active area of the device was 1.0 cm$^2$.

### 2.7 Characterization and measurements

The optical absorbance from 400 nm to 800 nm were obtained using ultraviolet-visible spectroscopy (UV-Vis) (Lambda 25, Perkin Elmer). The functional group of the dyes was examined using FTIR (Thermo Scientific Nicolet 6700; software: OMNIC 8). The surface shape and elemental content of $TiO_2$ nanoparticles were performed using Field Emission- Scanning Electron Microscopy (FE-SEM - Model Nova NanoSEM 450, Thermo Fisher). A confocal Micro-Raman Imaging System (Horiba XploRA Plus, UK) instrument with the wavelength of 525 nm was used to acquire Raman spectra of the samples. The thickness of the annealed sample was measured using a Surface Profiler (Veeco, Dektak 150).

### 2.8 DSSC photo-conversion efficiency, PCE

The photovoltaic DSSC parameters were examined using a Keithley source meter (Model: 4200 SCS), under a simulated solar light power supply (AM 1.5, 100 mW/cm$^2$) provided by a simulator (Oriel, 91160-1000). The active area was 1.0 cm$^2$. The open-circuit voltage (Voc), short circuit current density (Jsc), and fill factor (FF) were used to characterise the photovoltaic performance of the solar panels. The fill factor (FF) was calculated based on the I-V curve using formula (1) [25].

$$FF = (Imax \times Vmax) \div (Isc \times Voc) \quad (1)$$

Where, Imax and Vmax are the maximum current-density and maximum voltage for Pmax (maximum power output), Isc is the short-circuit current and Voc is the open-circuit photovoltage respectively. The total conversion efficiency (η) of a solar cell is calculated through equation (2)[26].

$$\text{Efficiency}, \eta = ( J_{sc} \times V_{oc} \times FF \div P_{in} ) \quad (2)$$

Where Pin is the incident light power on the cell and Jsc is the short-circuit current density.

## 3. RESULTS AND DISCUSSION

### 3.1 FESEM and EDX analysis

#### 3.1.1 FESEM analysis

The surface morphologies of the pure $TiO_2$ and $MgSO_4$-doped $TiO_2$ were probed by Field Emission Scanning Electron Microscopy (FESEM) and the images are shown in Figure 2 (a) and Figure 2 (b). The formation of a nanoporous structure with average nanoparticles of 25 nm was identified using a 400 nm scale TLD detector. As can be noted, the comparison of the two images indicates that the morphology of the undoped surface exhibits a slightly porous structure compared to the doped surface. This phenomenon may arise from the integration of magnesium sulfate ($MgSO_4$) granules, which adhere to the surface of titanium dioxide ($TiO_2$) resulting in a more compact surface structure. The $MgSO_4$-doped $TiO_2$ film has lesser pores with network appears to be more interconnected which can be attributed to the addition of dopant into the anatase lattice of $TiO_2$.

Secondly, it can be observed that the size of most particles in Figure 2(a) was 25 nm, however in Figure 2(b), some of the particles were mixed ranging from 35 nm to 40 nm. M. Rashad et al.[27], revealed that the particle size of Mg can be varied from 30 nm to 50 nm, while the particle size of $TiO_2$ ranges from 20 nm to 25 nm. It is also known that metal ions could be easily substituted into the $TiO_2$ lattice if their ionic radii were comparable to the Ti4+ cations [30]. This indicated that the larger particles, which were considered to be Mg particles, were effectively deposited on the $TiO_2$ surface [28]. The formation of a porous $TiO_2$ photoanode is crucial for the fabrication of high-performance DSSCs, as it offers a high specific surface area for dye adsorption and allows for deep infiltration of the liquid electrolyte. The size of the pores in $TiO_2$ particles influences the characteristics of dye adsorption and electrolyte diffusion. The $TiO_2$ photoanodes created with porous particles are anticipated to enhance the dye loading on the electrodes and improve the transport of the electrolyte, consequently boosting the efficiency of the DSSCs. [29].

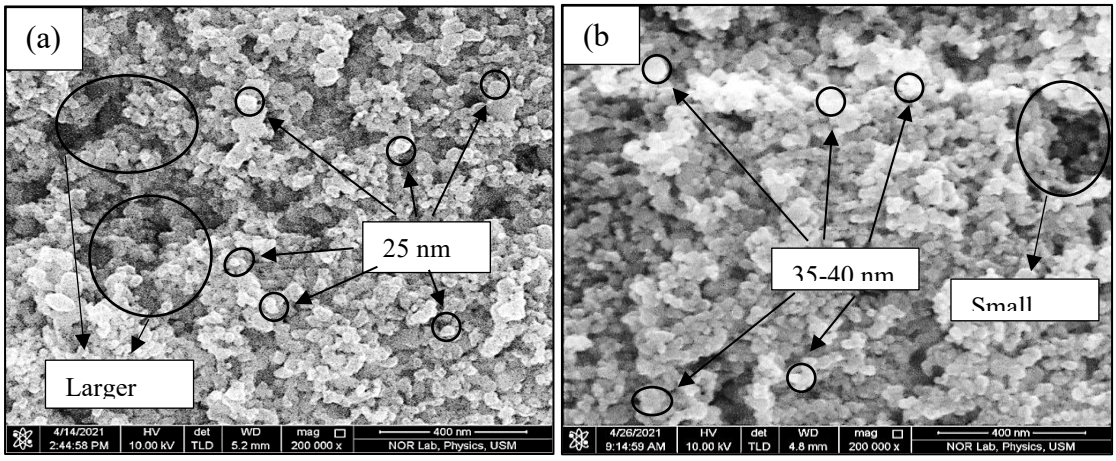


**Fig. 2.** FE-SEM images of **(a)** Pure $TiO_2$, **(b)** $MgSO_4$-doped $TiO_2$ films at 200,000× magnification

### 3.1.2 EDX Analysis

The EDX spectra and chemical composition of pure $TiO_2$ and Mg-doped $TiO_2$ thin films are shown in Figure 3, and their elementals composition are summarised in Table 1. The elemental composition analysis performed clearly shows the presence of magnesium in the $MgSO_4$-doped $TiO_2$ sample together with the leading component Ti and O.

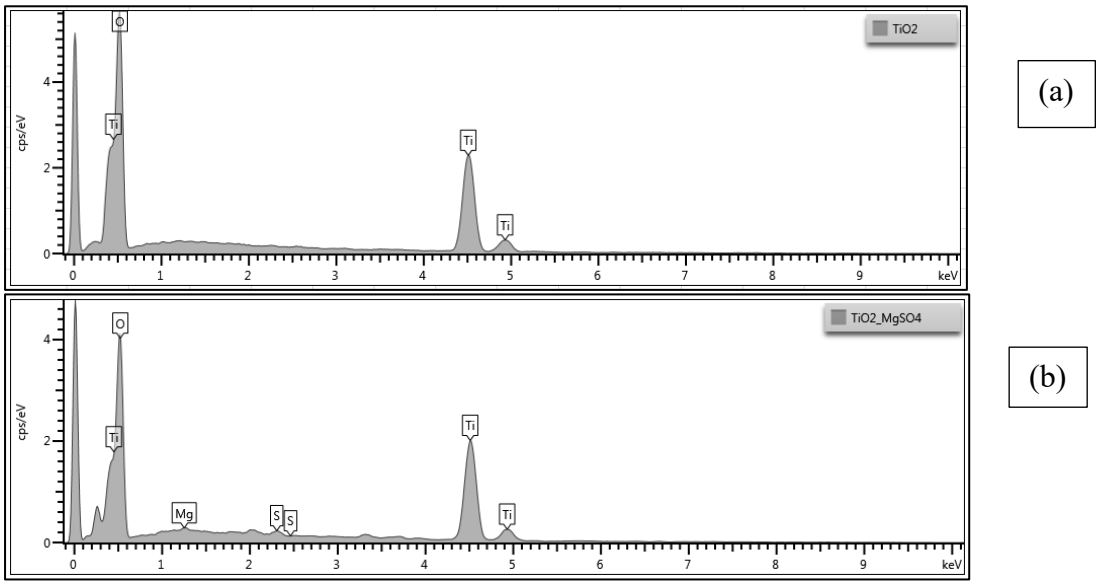


**Fig. 3.** EDX spectra of **(a)** Pure $TiO_2$ and **(b)** $MgSO_4$-doped $TiO_2$

**Table 1** EDX analysis for the Pure $TiO_2$ and $MgSO_4$-doped $TiO_2$ particles

| **$TiO_2$** | | | |
|---|---|---|---|
| Elements | at % | | wt% |
| O | 60.02 | | 33.40 |
| Ti | 39.98 | | 66.60 |
| **Total** | **100** | | **100** |
| | | | |
| Elements | at % | | wt % |
| O | 57.59 | | 31.67 |
| Ti | 40.21 | | 66.20 |
| Mg | 1.20 | | 0.92 |
| S | 1.00 | | 1.21 |
| **Total** | **100** | | **100** |

Meanwhile, for pure $TiO_2$ photoelectrode, the atomic percentages of Ti and O are 39.98 % and 60.02 %, respectively. Because of the bonding chemical formula of $TiO_2$, the data shows that oxygen has a higher mass than Ti (O - Ti – O). Moreover, the analysis of both samples reveals that the $TiO_2$ nanoparticles are completely free from any external impurities, confirming their exceptional purity and suitability for use as photo materials with natural dye [31,32].

### 3.2 Raman analysis

Ohsaka et al. [33] reported that $TiO_2$ anatase phase contains six Raman active modes (designated $A_{1g}$ +$B_{1g}$ +$E_{g)}$, two infrared (IR) active modes (designated $A_{2u}$ and $E_u$) and a silent mode (designated $B_{2u}$). However, in this study, the modes that appeared in both samples are Raman active modes which can be observed at 133 (Eg), 389 (Eg), 504 ($A_{1g}$), 506 ($A_{1g}$) and 631 (Eg) $cm^{-1}$. These modes are assigned to the Eg and $A_{1g}$ modes as reported by Alamgir and co-workers [34].

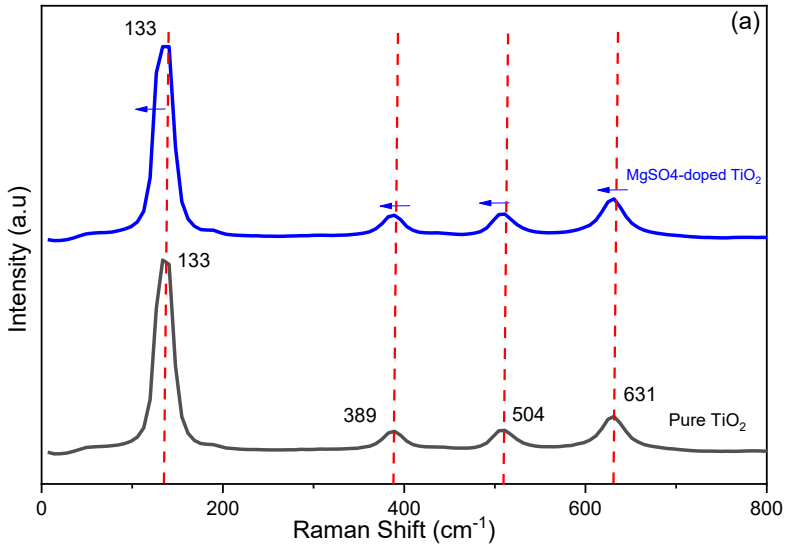


**Fig. 4.** Raman spectra for pure $TiO_2$ and $MgSO_4$-doped $TiO_2$

To further confirm that $MgSO_4$ is incorporated into the framework of anatase $TiO_2$, Raman spectroscopy for the sample is also studied in the range of 100-800 $cm^{-1}$. In this section, only two measurements are displayed; nevertheless, the other two parameters for $TiO_2$-$MgSO_4$-A and $MgSO_4$-doped $TiO_2$-A) were negligible. Figure 4 demonstrates the typical spectra Raman of anatase $TiO_2$ with four vibrational bands at 133, 389,504, and 631 $cm^{-1}$, conforming with the literature reported [34]. Meanwhile, the Raman vibrational peaks of $MgSO_4$-doped$TiO_2$ were observed at 133 (Eg),389 (Eg),506 ($A_{1g}$) and 631(Eg) $cm^{-1}$ respectively. The effective doping of $TiO_2$ film with $MgSO_4$ is evidenced by the blue-shift peak position observed in Raman spectroscopy. In addition, it also indicates a significant distortion in the original anatase lattice is occurring due to Mg substitution [35]. In a nutshell magnesium ions have been integrated into the $TiO_2$ lattice and framework of $TiO_2$ anatase. Furthermore, it is also noticed that the increase in crystallite size and peak intensity upon doping also suggests the successful incorporation of $MgSO_4$ into the $TiO_2$ film which was supported by previous EDX results.

### 3.3 UV-Visible Spectroscopy Analysis

The absorption spectra of four different dye solutions (after dye immersing process) were analyzed using UV–Vis spectroscopy in the range of 400–800 nm wavelength and their spectra were presented in Figure 5 (a). It could be noticed that all of the post immersion dye samples containing $MgSO_4$, whether as a doping agent or additive, exhibited higher and a red shift in the absorption, and these were primarily attributed to the Mg doping [28].

Having absorption in the visible spectrum indicates that the MS dye was suitably used as a photosensitiser in DSSC applications. The enhanced light absorption of the dye solutions containing $MgSO_4$ were basically due to the decreases in the HOMO-LUMO energy levels of the dye, which makes it easier for electrons to jump from valence to the conduction band [36]. Due to the direct application of $MgSO_4$ into the dye solution, the highest peak in visible light absorption were observed in the $MgSO_4$-doped $TiO_2$-A thin film and $TiO_2$-$MgSO_4$-A. Another possible reason for the higher UV peak position were due to the pH level of both solutions, which became more acidic after the dissolution of the $MgSO_4$ additive. Dissolution process increased the levels of free positive hydrogen ions (protonation) and enhanced the acidity of the dye solutions, consistent with observations documented in earlier studies [24]. Moreover, the addition of $MgSO_4$ to $TiO_2$-A and $TiO_2$-$MgSO_4$-A led to a broader visible range, thereby improving the effectiveness of light energy conversion into photo-generated electrons [24].

The increased acidity of the dye solutions due to dissolution was accompanied by an enhancement in the bandgap, Eg, of the dye molecules, which is linked to a higher LUMO. The higher LUMO level of the dye facilitates more rapid electron injection within the system. The Tauc plot technique stands out as one of the most effective approaches for ascertaining the bandgap energy of the dye solution. The determination of Eg was carried out using the equation (3) [37], derived from the previously plotted ultraviolet-visible data. Meanwhile Figure 5 (b) illustrated the band gaps of $TiO_2$, $TiO_2$-$MgSO_4$-A, $MgSO_4$-doped $TiO_2$ and $MgSO_4$-doped $TiO_2$-A thin films, respectively.

$$\alpha h\nu = A(h\nu - Eg)^n \quad (3)$$

where α is the absorption coefficient, $h\nu$ is the photon energy, A is a constant, Eg is the optical bandgap and n denotes the electronic transition, whereby n=2 is direct allowed transitions. The calculated bandgap energies are given in Table 2 and the values of the bandgap were in the range of 1.814 eV to 1.823 eV. The Eg values for $TiO_2$ and $TiO_2$-$MgSO_4$-A obtained from the graph were found to be 1.814 eV to 1.820 eV. Meanwhile, the Eg values for $MgSO_4$-doped $TiO_2$ and $MgSO_4$-doped $TiO_2$-A were 1.818 eV and 1.823 eV, respectively.

The bandgap exhibited an increase from 1.814 eV to 1.818 eV following the doping process. The presence of the $Mg^{2+}$ dopant leads to the formation of oxygen vacancies, which are directly associated with the absorption and transportation of photons within the $TiO_2$ structure [38]. This finding suggests that there is an enhancement in

photon absorption of the film as a consequence of Mg doping. Therefore, improving the light absorption of the photoanode is a viable approach to enhance the performance of dye-sensitised solar cells [39]. Moreover, it also indicates a strong correlation between doping and photon absorption, suggesting that $MgSO_4$-doped $TiO_2$-A is capable of harvesting a greater amount of visible light to the cell. This enhancement may be due to the multiple reflections of incoming light within the host structure ($TiO_2$) and the formation of additional energy levels situated within the bandgap [40]. The additional energy level formed within the bandgap arises from the movement of the Fermi energy level of $Mg^{2+}$ towards the valence band, resulting in the formation of a P-type semiconductor [41].

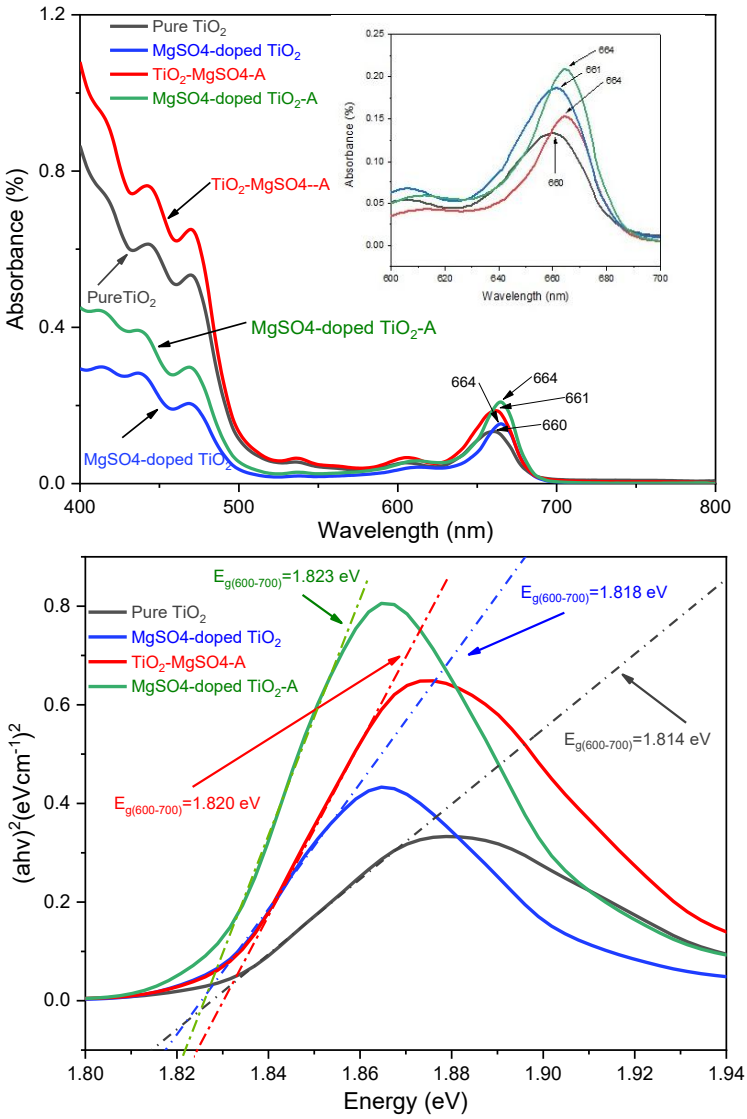


**Fig. 5 (a)** Absorption spectra of different photoanodes extracted with Mitragyna speciosa in methanol (inset pic is the absorption spectra between 600-700 nm), **(b)** Tauc plot of various photoanodes

**Table 2** Optical energy bandgap of different photoanodes

| Samples | Absorption wavelength (nm) | Optical energy gap (eV) |
|---|---|---|
| Pure $TiO_2$ | 600-700 | 1.814 |
| $MgSO_4$-doped $TiO_2$ | 600-700 | 1.818 |
| $TiO_2$-MgSO4-A | 600-700 | 1.820 |
| $MgSO_4$-doped $TiO_2$-A | 600-700 | 1.823 |

### 3.4 Fourier-Transform Infrared (FTIR) Spectra Analysis

Figure 6 illustrates the FTIR transmission spectra of the post-immersion dye solutions (identical samples utilized in the UV-Vis measurement), recorded within the range of 400–4000 $cm^{-1}$. It is evident that nearly all the significant functional groups of the dye sensitizer, including O-H, C-H, C=O, and C-O, were present. The O-H group emerges as the broadest peak at 3257 $cm^{-1}$, and its normally dictates the capability of dye adsorption on $TiO_2$ nanoparticles. It can be noticed that the $MgSO_4$ treated dye sensitizer immersed with $MgSO_4$-doped $TiO_2$-$MgSO_4$-A has contributed to the highest O-H content in the respective dyes. This situation is closely related to the

increased number of O-H and $Mg^{2+}$ produced during $MgSO_4$ dissolution process with water in those two samples (samples with added $MgSO_4$ additive).
It was reported that the O-H group is important constituent for chelating with the $TiO_2$ film on the surface of the conducting glass [42]. Moreover, O-H group plays a key role in improvement of photocatalytic activity [43] which is owing to the ability of the hydroxyl group to capture the photo-excited electron.

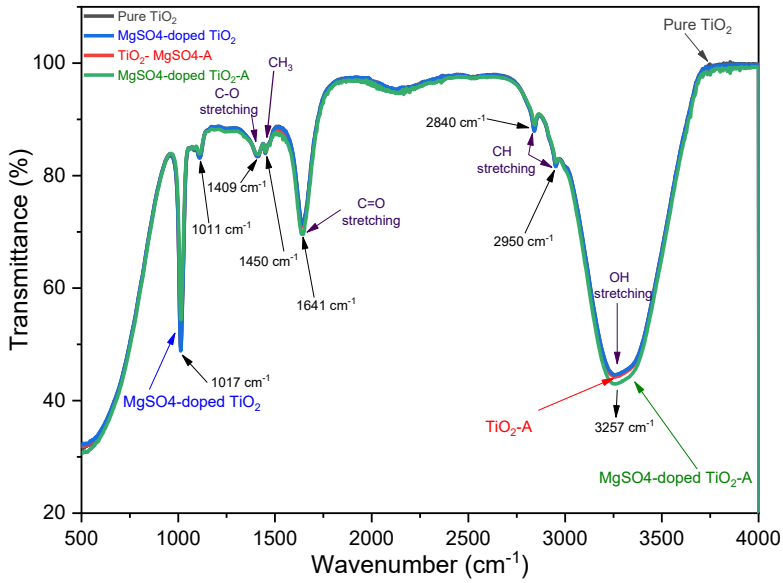


**Fig. 6.** FTIR spectra of Pure $TiO_2$, $TiO_2$-A, $MgSO_4$-doped $TiO_2$ and $MgSO_4$-doped $TiO_2$-A
The peaks lying at 2840 $cm^{-1}$ and 2950 $cm^{-1}$ represent the functional group corresponding to the C−H symmetric and antisymmetric stretching modes. The carbonyl functional group signature of all samples was present between 1500 $cm^{-1}$ to 2000 $cm^{-1}$ and the peak at 1641 $cm^{-1}$ was attributed to the stretching of the carbonyl group (C=O). The C=O enables the chlorophyll pigment to anchor to the $TiO_2$ [44]. Meanwhile, the $CH_3$ group at 1450 $cm^{-1}$ slightly differed in terms of transmittance intensity and C-O stretching was discovered at 1409 $cm^{-1}$. It was reported that the organic sulfate bonding normally occurs between 1000 $cm^{-1}$ to 1200 $cm^{-1}$ [45]. The absorption band at 1000 $cm^{-1}$ are related to S=O [46], however in this research the absorption bands can be ascribed at 1011 $cm^{-1}$ and 1017 $cm^{-1}$. This may be caused by the interaction and combined absorption of sulfate ions ($SO_4^{2-}$) with the chlorophyll dye. Moreover, these frequencies are known as unique fingerprints due to the presence of sulfate salts.
The hydroxyl and carbonyl groups of sample with $MgSO_4$ were found to be more intense than pure $TiO_2$. It was reported that the presence of additional hydroxyl and carbonyl groups in the dye solution was found to improve dye adsorption on the $TiO_2$. In addition, the red-shifted absorption peak (highest peak) for dyes adsorbed on $TiO_2$ is caused by strong chemical bonds between the adsorbed dye molecules and the $TiO_2$ surface [47].

**3.5 Photovoltaic performance**

Figure 7(a) illustrates the I-V characteristics of various dry cells produced via different techniques (either additive/doping $MgSO_4$) in comparison to the pure-$TiO_2$ photoelectrode. As regards to the $MgSO_4$ treated (doped or additive) photoelectrode, at any point of anode voltage (V), the current (I) was always higher compared to the current of the untreated pure-$TiO_2$. The increased current indicates that the interfacial resistance of $MgSO_4$-doped $TiO_2$ additive is lower than those of pure $TiO_2$, attributable to $Mg^{2+}$ doping. Multiple preceding studies on doping $TiO_2$ confirmed that the incorporation of a dopant enhances the conductivity of solid-state DSSCs and influences the device's efficiency. Moreover, doping significantly reduces the recombination loss [52], and with the optimal doping level, the conductivity of $TiO_2$ can be improved [53][54]. The enhancement in conductivity proved advantageous for applications in optoelectronics, photocatalysis, and microelectronics [55][56].
Figure 7(b) shows the photocurrent-voltage curves of several DSSC cells under light intensity of 100 $mW/cm^2$ at AM1.5. Meanwhile, their photovoltaic characteristics were summarised in Table 3. For the DSSC without any additional treatment (pure $TiO_2$), the photocurrent density, Jsc open-circuit voltage, Voc, fill factor, FF and the overall efficiency, η were 1.67 mA /$cm^2$, 530 mV, 33.00% and 0.29%, respectively. The pure $TiO_2$ cell exhibited the lowest efficiency compared to other DSSCs, likely due to reduced dye adsorption and the loss of photogenerated electrons resulting from recombination. Generally, untreated $TiO_2$ photoelectrodes and untreated dye molecules exhibit elevated interfacial/interlayer resistances and reduced photocatalytic activity (reduced dye adsorption), respectively. In the interim, the overall efficiency of the cells subjected to single treatments ($MgSO_4$-doped $TiO_2$ and $TiO_2$-MgSO4-A) exhibited marginally superior Jsc and Voc values in comparison to the pure $TiO_2$ cell. The slight increase of Jsc and Voc were probably attributed to the impact of the individual treatment imposed to the cell, either the passivation layer or dye adsorption enhance the additive. However, for the case of combined treatment in the $MgSO_4$-doped $TiO_2$-A cell. The combined treatment's cell has a maximum efficiency of 0.86 %, and Jsc, Voc, and FF, were 3.38 mA/$cm^2$, 570 mV and 44.70 %, respectively. This clearly implies that,

the higher Jsc and Voc were attributed to more dye loading (higher dye adsorption) and reduced recombination of the photogenerated electrons (effective interface passivation) achieved due to the introduction of $MgSO_4$ as a dopant and additive combined.

Moreover, the elevated fill factor of the dye-sensitized solar cell signifies effective interaction among the cell's components. DSSCs including $MgSO_4$ as a dopant and additive demonstrate a fill factor of 44.70 %, which is comparatively high comparable to other cells. This indicates that $MgSO_4$-doped $TiO_2$ with dye additives and electrolytes exhibits a favorable interaction with chlorophyll molecules. Furthermore, the inclusion of $MgSO_4$ as a dopant significantly augmented the carbonyl and hydroxyl groups in the dye, facilitating the effective chelation of titanium ions on the thin film surface. Moreover, the addition of $MgSO_4$ salt to the chlorophyll dye molecules resulted in the formation of sulfur monoxide (S=O) and magnesium oxide (Mg-O) linkages on the $TiO_2$ layer. [51]. Furthermore, effective contact among $MgSO_4$-doped $TiO_2$, dye additive, and electrolyte facilitates the seamless passage of electrons to each component, yielding a high Jsc and FF. The efficiency (η) of dye-sensitized solar cells (DSSC) is directly related to the open-circuit voltage (Voc), short-circuit current density (Jsc), and fill factor (FF). The efficiency of DSSCs is enhanced when the Voc, Jsc, and FF parameters are elevated. The DSSC incorporating $MgSO_4$-doped $TiO_2$-A exhibits the maximum efficiency (η) of 0.86 %.

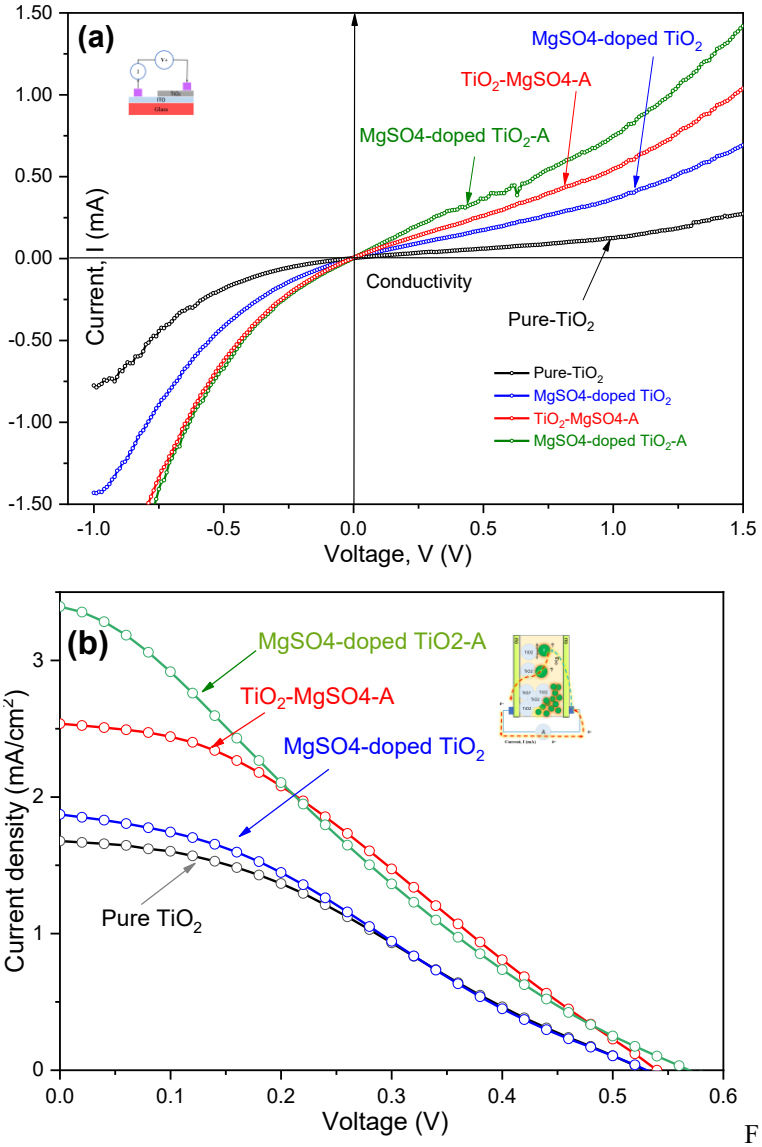


F

**Fig. 7 (a)** Current vs voltage (IV) produced via different techniques **(b)** Photocurrent-voltage characteristics of DSSCs fabricated with Pure $TiO_2$, $TiO_2$-A, $MgTiO_2$ and $MgTiO_2$-A photoelectrodes

**Table 3** Solar energy conversion efficiency of the DSSC based on different photoelectrodes

| Working electrode | Jsc (mA/cm$^2$) | Voc (mV) | FF (%) | η (%) |
|---|---|---|---|---|
| Pure $TiO_2$ | 1.67 | 530 | 33.00 | 0.29 |
| $MgSO_4$-doped $TiO_2$ | 1.87 | 530 | 32.60 | 0.32 |
| $TiO_2$-MgSO4-A | 2.52 | 540 | 30.60 | 0.42 |
| $MgSO_4$-doped $TiO_2$-A | 3.38 | 570 | 44.70 | 0.86 |

## 4. CONCLUSION

In this research, the combined treatment procedure using $MgSO_4$ as passivation layer and also as dye additive in the fabrication of DSSC has been successfully investigated. Upon incorporating $Mg^{2+}$ ions into the $TiO_2$ lattice, highly crystallized and well-oriented $TiO_2$ crystals are successfully fabricated. Also, $MgSO_4$-doped $TiO_2$ demonstrates a mixed size nanoparticles with much larger grains at fewer grain boundaries compared to the homogenous surface morphology of the pure $TiO_2$. As a result, a larger size of $MgSO_4$ mixed with slightly smaller $TiO_2$ nanoparticles enhanced the PCE of the cells through light scattering. Furthermore, the successfulness of doping process has been demonstrated by the blue-shift peak position in Raman spectroscopy measurement and higher conductivity of the dry cell. Meanwhile, the bandgap was found to increase from 1.814 eV to 1.820 eV from $TiO_2$ to $TiO_2$-MgSO4-A. As for $MgSO_4$- doped $TiO_2$ the bandgap was 1.818 eV and led to a further increase to 1.823 eV for $MgSO_4$-doped $TiO_2$-A. Higher Eg offers faster electron injection from LUMO to CB of the $TiO_2$. Also, the FTIR spectroscopy has evidence the existence of all important functional groups of dye sensitizer such as O-H, C-O and C=O which were important for dye attachment to the $TiO_2$ nanoparticles. At some point, the utilization of $MgSO_4$ as both a dopant and an additive resulted in an enhancement of photoconversion efficiency, increasing from 0.29 % to 0.86 % in comparison to pure $TiO_2$. The observed trend may be attributed to the enhancement of Jsc resulting from improvements in dye adsorption and the reduction of interfacial resistance within the porous $TiO_2$ film. This may inhibit the recombination occurring on the $TiO_2$ surface, thereby improving the performance of Voc. The findings demonstrate that employing $MgSO_4$ as a dual-purpose agent, both as a dopant and an additive, has concurrently enhanced the overall performance of the dye-sensitized solar cells.

**Acknowledgements**
The authors thank Universiti Teknologi Mara (UiTM) Permatang Pauh, Pulau Pinang and Universiti Sains Malaysia (USM), Pulau Pinang for their research facilities. This research is financially supported by the Ministry of Higher Education of Malaysia (MOHE) through Fundamental Research Grant Scheme (FRGS-2019-1) (ID no 284362-301651).

## REFERENCES

[1] Mathew, Simon, Aswani Yella, Peng Gao, Robin Humphry-Baker, Basile FE Curchod, Negar Ashari-Astani, Ivano Tavernelli, Ursula Rothlisberger, Md Khaja Nazeeruddin, and Michael Grätzel. "Dye-sensitized solar cells with 13% efficiency achieved through the molecular engineering of porphyrin sensitizers." Nature chemistry 6, no. 3 (2014): 242-247. https://doi.org/10.1038/nchem.1861
[2] Grätzel, Michael. "A Low-cost, High-efficiency Solar Cell Based on Dye-sensitized Colloidal TiO2 Films." Nature 353, no. 6346 (1991): 737-740. https://doi.org/10.1038/353737a0.
[3] Grätzel, Michael. "Recent advances in sensitized mesoscopic solar cells." Accounts of chemical research 42 11 (2009): 1788-98 . https://doi.org/10.1021/ar900141y
[4] Nazeeruddin, Mohammad K., Peter Pechy, Thierry Renouard, Shaik M. Zakeeruddin, Robin Humphry-Baker, Pascal Comte, Paul Liska et al. "Engineering of efficient panchromatic sensitizers for nanocrystalline TiO2-based solar cells." Journal of the American Chemical Society 123, no. 8 (2001): 1613-1624. https://doi.org/10.1021/ja003299u
[5] Sofyan, Nofrijon, Aga Ridhova, Akhmad Herman Yuwono, and Arief Udhiarto. "Fabrication of solar cells with TiO2 nanoparticles sensitized using natural dye extracted from mangosteen pericarps." International Journal of Technology 8, no. 7 (2017): 1229-1238. https://doi.org/10.14716/ijtech.v8i6.692
[6] Jarernboon, Wirat, Samuk Pimanpang, Santi Maensiri, Ekaphan Swatsitang, and Vittaya Amornkitbamrung. "Optimization of titanium dioxide film prepared by electrophoretic deposition for dye-sensitized solar cell application." Thin Solid Films 517, no. 16 (2009): 4663-4667. https://doi.org/10.1016/j.tsf.2009.02.129
[7] Odobel, Fabrice, Loïc Le Pleux, Yann Pellegrin, and Errol Blart. "New photovoltaic devices based on the sensitization of p-type semiconductors: challenges and opportunities." Accounts of chemical research 43, no. 8 (2010): 1063-1071. https://doi.org/10.1021/ar900275b
[8] Duta, M., S. Simeonov, V. Teodorescu, L. Predoana, S. Preda, M. Nicolescu, A. Marin et al. "Structural and electrical properties of Nb doped TiO2 films prepared by the sol–gel layer-by-layer technique." Materials Research Bulletin 74 (2016): 15-20. https://doi.org/10.1016/j.materresbull.2015.10.009
[9] Rehman, Shama, Ruh Ullah, AwM Butt, and N. D. Gohar. "Strategies of making TiO2 and ZnO visible light active." Journal of hazardous materials 170, no. 2-3 (2009): 560-569. https://doi.org/10.1016/j.jhazmat.2009.05.064
[10] Zhang, Qifeng, Christopher S. Dandeneau, Stephanie Candelaria, Dawei Liu, Betzaida B. Garcia, Xiaoyuan Zhou, Yoon-Ha Jeong, and Guozhong Cao. "Effects of lithium ions on dye-sensitized ZnO aggregate solar cells." Chemistry of Materials 22, no. 8 (2010): 2427-2433. https://doi.org/10.1021/cm9009942
[11] Shakir, Sehar, Hafiz M. Abd-ur-Rehman, Kamran Yunus, Mitsumasa Iwamoto, and Vengadesh Periasamy. "Fabrication of un-doped and magnesium doped TiO2 films by aerosol assisted chemical vapor deposition for dye sensitized solar cells." Journal of Alloys and Compounds 737 (2018): 740-747. https://doi.org/10.1016/j.jallcom.2017.12.165

[12] Athira, K., K. T. Merin, T. Raguram, and K. S. Rajni. "Synthesis and characterization of Mg doped TiO2 nanoparticles for photocatalytic applications." Materials Today: Proceedings 33 (2020): 2321-2327. https://doi.org/10.1016/j.matpr.2020.04.580
[13] Qiu, Weiming, Marie Buffière, Guy Brammertz, Ulrich W. Paetzold, Ludo Froyen, Paul Heremans, and David Cheyns. "High efficiency perovskite solar cells using a PCBM/ZnO double electron transport layer and a short air-aging step." Organic electronics 26 (2015): 30-35. https://doi.org/10.1016/j.orgel.2015.06.046
[14] A. El Hamidi, M. Chaik, T. Jannane, K. Meziane, A. El Hichou, and A. Almaggoussi, "Effect of Mg Doping on Structural and Optical Properties of Al-Mg Co-doped ZnO Thin Films Deposited via Sol-gel Technique," Res. Rev. J. Mater. Sci. 06, no. 02 (2018): 99-109. https://doi.org/10.4172/2321-6212.1000221
[15] Xiao, Fang, Xuexia Song, Zhaohui Li, Honglai Zhang, Lingjun Zhang, Gangtie Lei, Qizhen Xiao, Zhongliang Hu, and Yanhuai Ding. "Embedding of Mg-doped V 2 O 5 nanoparticles in a carbon matrix to improve their electrochemical properties for high-energy rechargeable lithium batteries." Journal of Materials Chemistry A 5, no. 33 (2017): 17432-17441. https://doi.org/10.1039/C7TA02761C
[16] Arof, S., Noorsal, E., Yahaya, S. Z., Hussain, Z., Mohd Ali, Y., Abdullah, M. H., & Safie, M. K. (2023). Adaptive sliding mode feedback control algorithm for a nonlinear knee extension model. Machines, 11(7), 732.
[17] Abdullah, M. H., et al. "Synergistic effect of complementary organic dye co-sensitizers for potential panchromatic light-harvesting of dye-sensitized solar cells." Optical Materials 133 (2022): 113016.
[18] Senge, Mathias O., and Stuart A. MacGowan. "The structural chemistry of isolated chlorophylls." Handbook of porphyrin science 13 (2010): 253-297.
[19] Kuo, Chin-Guo, and Bee-Jeng Sheen. "Seaweed Chlorophyll on the Light-electron Efficiency of DSSC." Journal of the Chinese Chemical Society 58, no. 2 (2011): 186-190. https://doi.org/10.1002/jccs.201190075
[20] Calogero, Giuseppe, Gaetano Di Marco, Stefano Caramori, Silvia Cazzanti, Roberto Argazzi, and Carlo Alberto Bignozzi. "Natural dye senstizers for photoelectrochemical cells." Energy & Environmental Science 2, no. 11 (2009): 1162-1172. https://doi.org/10.1039/B913248C
[21] Ahmad Khan, Azlina, M. H. Abdullah, Faizal Rahman, Syarifah Yusof, Mohamad Hafiz bin Mamat, Afaf Radzol, Diyana Md Sin, Hayati Sabani, Shameen Banu IB, and M. Rusop. "Synergistic Impact of Magnesium Compound as a Potential Dye Additive for Organic-Based Sensitizer in Dsscs. https://doi.org/10.1016/j.mtcomm.2022.105259
[22] Khan, A. A., M. H. Abdullah, M. D. A. Hassan, M. K. Osman, A. F. A. Rahim, M. H. Mamat, MY Syarifah Adilah, and I. B. S. Banu. "Co-active impact of surface hydroxyls on the solvation shell and dye adsorption of Mitragyna Speciosa chlorophyll molecules in dye-sensitised solar cells." Journal of the Iranian Chemical Society 20, no. 7 (2023): 1743-1756. https://doi.org/10.1007/s13738-023-02795-w
[23] Hölscher, Florian, Peer-Robin Trümper, Irén Juhász Junger, Eva Schwenzfeier-Hellkamp, and Andrea Ehrmann. "Application methods for graphite as catalyzer in dye-sensitized solar cells." Optik 178 (2019): 1276-1279. https://doi.org/10.1016/j.ijleo.2018.10.123
[24] Khan, A. A., MY Syarifah Adilah, M. H. Mamat, S. Z. Yahaya, S. Setumin, M. N. Ibrahim, K. Daud, and M. H. Abdullah. "Magnesium sulfate as a potential dye additive for chlorophyll-based organic sensitiser of the dye-sensitised solar cell (DSSC)." Spectrochimica Acta Part A: Molecular and Biomolecular Spectroscopy 274 (2022): 121140. https://doi.org/10.1016/j.saa.2022.121140
[25] Bashar, H., M. M. H. Bhuiyan, M. R. Hossain, F. Kabir, M. S. Rahaman, M. S. Manir, and T. Ikegami. "Study on combination of natural red and green dyes to improve the power conversion efficiency of dye sensitized solar cells." Optik 185 (2019): 620-625. https://doi.org/10.1016/j.ijleo.2019.03.043
[26] Ammar, Ahmed M., Hemdan SH Mohamed, Moataz MK Yousef, Ghada M. Abdel-Hafez, Ahmed S. Hassanien, and Ahmed SG Khalil. "Dye-sensitized solar cells (DSSCs) based on extracted natural dyes." Journal of Nanomaterials 2019, no. 1 (2019): 1867271. https://doi.org/10.1155/2019/1867271
[27] Rashad, Muhammad, Fusheng Pan, Aitao Tang, Muhammad Asif, Jia She, Jun Gou, Jianjun Mao, and Huanhuan Hu. "Development of magnesium-graphene nanoplatelets composite." Journal of composite materials 49, no. 3 (2015): 285-293. https://doi.org/10.1177/0021998313518
[28] Arshad, Zafar, Asif Hussain Khoja, Sehar Shakir, Asif Afzal, M. A. Mujtaba, Manzoore Elahi M. Soudagar, H. Fayaz, Sarah Farukh, and Mudassar Saeed. "Magnesium doped TiO2 as an efficient electron transport layer in perovskite solar cells." Case Studies in Thermal Engineering 26 (2021): 101101. https://doi.org/10.1016/j.csite.2021.101101
[29] Arka, Girija Nandan, Shashi Bhushan Prasad, and Subhash Singh. "Comprehensive study on dye sensitized solar cell in subsystem level to excel performance potential: A review." Solar Energy 226 (2021): 192-213. https://doi.org/10.1016/j.solener.2021.08.037
[30] Lyly Nyl, I., Aziz, A. F., Habibah, Z., Zaihidi, M. M., Abdullah, M. H., Herman, S. H., ... & Rusop, M. (2012). Optical properties and surface morphology of PMMA: TiO2 nanocomposite thin films. Advanced Materials Research, 364, 105-109.
[31] Ismail, L. N., Mohamad, N. N. H. N., Shamsudin, M. S., Zulkefle, H., Abdullah, M. H., Herman, S. H., & Rusop, M. (2012). Effect of solvent on the dielectric properties of nanocomposite poly (methyl methacrylate)-doped titanium dioxide dielectric films. Japanese Journal of Applied Physics, 51(6S), 06FG09.
[32] Shahrul, A. M., M. H. Abdullah, M. H. Mamat, MY Syarifah Adilah, A. A. A. Samat, I. H. Hamzah, M. A. Yusnita, and ZH Che Soh. "Synergistic role of aluminium sulphate flocculation agent as bi-functional dye

additive for Dye-Sensitized Solar Cell (DSSC)." Optik 258 (2022): 168945. https://doi.org/10.1016/j.ijleo.2022.168945
[33] Ohsaka, Toshiaki, Fujio Izumi, and Yoshinori Fujiki. "Raman spectrum of anatase, TiO2." Journal of Raman spectroscopy 7, no. 6 (1978): 321-324.
[34] Khan, Wasi, Shabbir Ahmad, M. Mehedi Hassan, and A. H. Naqvi. "Structural phase analysis, band gap tuning and fluorescence properties of Co doped TiO2 nanoparticles." Optical materials 38 (2014): 278-285. https://doi.org/10.1016/j.optmat.2014.10.054
[35] Iwantono, Iwantono, Fera Anggelina, Siti Khatijah Md Saad, Mohd Yusri Abd Rahman, and Akrajas Ali Umar. "Influence of Ag ion adsorption on the photoactivity of ZnO nanorods for dye-sensitized solar cell application." Materials Express 7, no. 4 (2017): 312-318. https://doi.org/10.1166/mex.2017.1380
[36] Ruess, Raffael, Sabina Scarabino, Andreas Ringleb, Kazuteru Nonomura, Nick Vlachopoulos, Anders Hagfeldt, Gunther Wittstock, and Derck Schlettwein. "Diverging surface reactions at TiO 2-or ZnO-based photoanodes in dye-sensitized solar cells." Physical Chemistry Chemical Physics 21, no. 24 (2019): 13047-13057. https://doi.org/10.1039/C9CP01215J
[37] Jiang, Yinhua, Fan Li, Yan Liu, Yuanzhi Hong, Peipei Liu, and Liang Ni. "Construction of TiO2 hollow nanosphere/g-C3N4 composites with superior visible-light photocatalytic activity and mechanism insight." Journal of Industrial and Engineering Chemistry 41 (2016): 130-140. https://doi.org/10.1016/j.jiec.2016.07.013
[38] Castro, Yolanda, Noemi Arconada, and Alicia Durán. "Synthesis and photocatalytic characterisation of mesoporous TiO2 films doped with Ca, W and N." Boletín de la Sociedad Española de Cerámica y Vidrio 54, no. 1 (2015): 11-20. https://doi.org/10.1016/j.bsecv.2015.02.003
[39] Guo, Kaimo, Meiya Li, Xiaoli Fang, Xiaolian Liu, Bobby Sebo, Yongdan Zhu, Zhongqiang Hu, and Xingzhong Zhao. "Preparation and enhanced properties of dye-sensitized solar cells by surface plasmon resonance of Ag nanoparticles in nanocomposite photoanode." Journal of power sources 230 (2013): 155-160. https://doi.org/10.1016/j.jpowsour.2012.12.079
[40] Subki, A. S. R. A., Mamat, M. H., Mohamed Zahidi, M., Abdullah, M. H., Shameem Banu, I. B., Vasimalai, N., ... & Mahmood, M. R. (2022). Optimization of aluminum dopant amalgamation immersion time on structural, electrical, and humidity-sensing attributes of pristine ZnO for flexible humidity sensor application. Chemosensors, 10(11), 489.
[41] Siva Rao, T., Teshome Abdo Segne, T. Susmitha, A. Balaram Kiran, and C. Subrahmanyam. "Photocatalytic degradation of dichlorvos in visible light by Mg2+-TiO2 nanocatalyst." Advances in Materials Science and Engineering 2012, no. 1 (2012): 168780. https://doi.org/10.1155/2012/168780
[42] Singh, Lakshmi K., and B. P. Koiry. "Natural dyes and their effect on efficiency of TiO2 based DSSCs: a comparative study." Materials Today: Proceedings 5, no. 1 (2018): 2112-2122. https://doi.org/10.1016/j.matpr.2017.09.208
[43] El Mir, L. "Luminescence properties of calcium doped zinc oxide nanoparticles." Journal of Luminescence 186 (2017): 98-102. https://doi.org/10.1016/j.jlumin.2017.02.029
[44] Zakaria, Puteri Najihah Megat, Ikhwan Syafiq Mohd Noor, and Tan Winie. "Caulerpa lentillifera Seaweed Extract as Natural Sensitizer for Dye-Sensitized Solar Cell." In Macromolecular Symposia, vol. 407, no. 1, p. 2100359. 2023. https://doi.org/10.1002/masy.202100359
[45] Coates, John. "Interpretation of infrared spectra, a practical approach." Encyclopedia of analytical chemistry 12 (2000): 10815-10837.
[46] Chaban, Galina M., Winifred M. Huo, and Timothy J. Lee. "Theoretical study of infrared and Raman spectra of hydrated magnesium sulfate salts." The Journal of chemical physics 117, no. 6 (2002): 2532-2537. https://doi.org/10.1063/1.1489997
[47] Zhang, Ming-Dao, Hai-Xian Xie, Xue-Hai Ju, Ling Qin, Qing-Xiang Yang, He-Gen Zheng, and Xing-Fu Zhou. "DD-π-A organic dyes containing 4, 4′-di (2-thienyl) triphenylamine moiety for efficient dye-sensitized solar cells." Physical Chemistry Chemical Physics 15, no. 2 (2013): 634-641. https://doi.org/10.1039/C2CP42993D
[48] Bisquert, Juan, Arie Zaban, Miri Greenshtein, and Iván Mora-Seró. "Determination of rate constants for charge transfer and the distribution of semiconductor and electrolyte electronic energy levels in dye-sensitized solar cells by open-circuit photovoltage decay method." Journal of the American Chemical Society 126, no. 41 (2004): 13550-13559. https://doi.org/10.1021/ja047311k
[49] Fan, Ke, Wei Zhang, Tianyou Peng, Junnian Chen, and Fan Yang. "Application of TiO2 fusiform nanorods for dye-sensitized solar cells with significantly improved efficiency." The Journal of Physical Chemistry C 115, no. 34 (2011): 17213-17219. https://doi.org/10.1021/jp204725f
[50] Yu, Hua, Shanqing Zhang, Huijun Zhao, Geoffrey Will, and Porun Liu. "An efficient and low-cost TiO2 compact layer for performance improvement of dye-sensitized solar cells." Electrochimica Acta 54, no. 4 (2009): 1319-1324. https://doi.org/10.1016/j.electacta.2008.09.025
[51] Pramananda, Viqry, Teuku Aufar Hadyan Fityay, and Erni Misran. "Anthocyanin as natural dye in DSSC fabrication: A review." In IOP Conference Series: Materials Science and Engineering, vol. 1122, no. 1, p. 012104. IOP Publishing, 2021.
[52] Wijayarathna, T. R. C. K., G. M. L. P. Aponsu, Y. P. Y. P. Ariyasinghe, E. V. A. Premalal, G. K. R. Kumara, and K. Tennakone. "A high efficiency indoline-sensitized solar cell based on a nanocrystalline TiO2

surface doped with copper." Nanotechnology 19, no. 48 (2008): 485703.
[53] Kathalingam, A., Jin-Koo Rhee, and Sung-Hwan Han. "Effects of graphene counter electrode and CdSe quantum dots in TiO2 and ZnO on dye-sensitized solar cell performance." International journal of energy research 38, no. 5 (2014): 674-682. https://doi.org/10.1002/er.3179
[54] Rahman, M. Atowar. "Enhancing the photovoltaic performance of Cd-free Cu2ZnSnS4 heterojunction solar cells using SnS HTL and TiO2 ETL." Solar Energy 215 (2021): 64-76. https://doi.org/10.1016/j.solener.2020.12.020
[55] Nair, Sinitha B., Hilal Rahman, Julie Ann Joseph, Stephen K. Remillard, and Rachel Reena Philip. "Aluminium doping–a cost effective and super-fast method for low temperature crystallization of TiO 2 nanotubes." CrystEngComm 21, no. 1 (2019): 128-134. https://doi.org/10.1039/C8CE01834K
[56] Krishnakumar, Varadharajan, Singaram Boobas, Jeyaram Jayaprakash, Mani Rajaboopathi, Bing Han, and Marjatta Louhi-Kultanen. "Effect of Cu doping on TiO 2 nanoparticles and its photocatalytic activity under visible light." Journal of Materials Science: Materials in Electronics 27 (2016): 7438-7447. https://doi.org/10.1007/s10854-016-4720-1